MATERIALS PHYSICS AND MECHANICS RESEARCH ARTICLE

Submitted: February 29, 2024 **Revised: January 15, 2025** **Accepted: January 26, 2025**

Preparation and characterization of geopolymer/activated carbon composite materials used as a bone substitute material

A. Moonphukhiao[1], B. Samran[2], S. Chaiwichian[1]✉

[1] Rajamangala University of Technology Isan Sakonnakhon Campus, Phangkon, Sakonnakhon, Thailand

[2] Nakhon Phanom University, Muang District, Nakhon Phanom, Thailand

✉ saranyou530531117@gmail.com

ABSTRACT

Geopolymer/activated carbon composite materials were successfully prepared using alkaline activator solution to be a binder. The physical and mechanical properties of as-prepared samples were characterized through X-ray diffraction, scanning electron microscopy, transmission electron microscopy, Fourier transform infrared spectrometry and compressive strength techniques. Results revealed that geopolymer/activated carbon composite materials exhibited amorphous phase and spherical-like and plate-like morphologies. Fourier transform infrared spectrometry results indicated that after the geopolymerization reaction, the band at 977 cm^{-1} was shifted to lower wavenumber (975 cm^{-1}). This might be attributed to the interaction of aluminum atoms and the formation of higher cross-linking in silicate geopolymer structure. The compressive strength of geopolymer/activated carbon composite materials decreased with increasing amount of activated carbon in geopolymer. It was found that the concentration of 0.001 mol. % activated carbon introduced into geopolymer gave the highest strength compared with other samples.

KEYWORDS

geopolymer • activated carbon • alkaline activator • geopolymerization reaction

Acknowledgements. *The authors would like to gratefully thank the Department of Science and Mathematics, Faculty of Industry and Technology, Rajamangala University of Technology Isan, Phangkon, Sakon Nakon for support.*

Citation: Moonphukhiao A, Samran B, Chaiwichian S. Preparation and characterization of geopolymer/activated carbon composite materials used as a bone substitute material. *Materials Physics and Mechanics*. 2025;53(1): 150–158. http://dx.doi.org/10.18149/MPM.5312025_12

Introduction

A significant component of the human body consists of 206 bones. Each bone has different internal and external structures, such as leg bones, arm bones, hip bones, etc. [1,2]. However, these bones may not remain throughout a person's life, as they can be affected by various factors, such as accidents, bone diseases, and bone deterioration [2,3]. To date, artificial bones or bone substitute materials have become crucial in addressing bone-related issues. As a result, many researchers have focused on the development of artificial bones to create efficient bone substitute materials and to improve production technologies for faster and more accurate procedures. Artificial bones or bone substitute materials are typically made from various metals, such as stainless steel, titanium, titanium-cobalt alloys, and others [4], which can suffer from corrosion during long-term use. To overcome this limitation, researchers have been seeking alternative materials to replace metals. Geopolymer, first synthesized by Davidovits in the 1970s [5–7], is classified as an inorganic polymer. It is well-known as a green pozzolanic material,

© A. Moonphukhiao, B. Samran, S. Chaiwichian, 2025.
Publisher: Peter the Great St. Petersburg Polytechnic University
This is an open access article under the CC BY-NC 4.0 license (https://creativecommons.org/li-censes/by-nc/4.0/)

produced using waste materials as aluminosilicate sources combined with an alkaline activator solution [8–13]. Geopolymers are significant alternative materials and have drawn substantial interest in biomedical applications to replace metals due to their desirable properties, such as low greenhouse gas emissions, corrosion resistance and environmental sustainability [11,14,15]. However, a limitation of pure geopolymer is its low compressive strength. To address this issue, numerous efforts have focused on incorporating porous materials into geopolymer to improve its compressive strength. Recently, porous materials, such as zeolite and activated carbon, have gained popularity for enhancing the mechanical properties of geopolymers [16]. Activated carbon, in particular, is a naturally derived porous material widely used in industry as an adsorbent and catalyst for waste and gas purification [16,17]. Additionally, activated carbon possesses important mechanical properties, such as resistance to abrasion and attrition, making it suitable for integration with geopolymer to enhance its compressive strength.

In this study, geopolymer/activated carbon composite materials were prepared by using an alkaline activator solution as a binder, with activated carbon added to the geopolymer solution to form the composite. Furthermore, we investigated the effect of varying concentrations of activated carbon in the geopolymer on the mechanical properties, with the aim of utilizing these materials in biomedical applications in the future. The chemical properties of all the prepared samples were characterized using X-ray diffraction (XRD), scanning electron microscopy (SEM), transmission electron microscopy (TEM), and Fourier transform infrared spectroscopy (FTIR).

Materials and Methods

Activated carbon was made of coconut shell by using potassium hydroxide (KOH) as an activating agent during chemical activation process. Firstly, the natural coconut shell was cleanly washed with deionized water to eliminate the contaminant. The coconut shell was then dried at 80 °C for 24 h in an electric oven to remove the water content. Next, the coconut shell was heated at 200 °C to form charcoal. The as-prepared charcoal was ground into small pieces and soaked in 6M KOH solution to generate porous volume. Then, the obtained suspension was filtered and washed with deionized water until pH 7 by using a centrifuge to split the particle and solution. Finally, the as-prepared activated carbon particles were dried in an electric oven at a temperature of 80 °C for 24 h and then heated at the calcination temperature of 600 °C for 1 h.

Geopolymer was prepared by using kaolin, CaO, NaOH and Na_2SiO_3 as precursor. First of all, kaolin was heated at 600 °C within 2 h to form metakaolin. Then, 2:1:1:1 of metakaolin, CaO, NaOH and Na_2SiO_3, respectively, was slowly dissolved in 25 ml of deionized water until becoming homogeneous solution. The as-prepared suspension was poured in the mold and dried at room temperature for 24 h. Finally, geopolymer for bone substitute materials was heated at 550 °C for 6 h.

Geopolymer/activated carbon composite materials were prepared by using NaOH as alkaline activator to activate geopolymer. 2:1:1:1 of metakaolin, CaO, NaOH and Na_2SiO_3, respectively, was dissolved in 25 ml of deionized water with vigorously magnetic stirrer till homogeneous solution. Then, the previously prepared activated carbon powders were added into the geopolymer solution with different mole ratios of 0.001 and 0.003 %

together with continuously magnetic stirring for 30 min. Next, the obtained suspension was poured in the mold, and then dried at room temperature overnight to construct a bone substitute material. The samples were finally heated at the high temperature of 550 °C for 6 h by a furnace.

The identification of phase structure of all samples was measured using X-ray diffraction (XRD, Philips X'Pert MPD, Thailand) with CuKα radiation (0.15418 nm) at the 2θ range of 10° to 80°. The morphology structure of as-prepared samples was studied via scanning electron microscopy (SEM, JEOL JSM-6335F, Thailand) technique. The microstructure and actual particle size of samples were investigated by using transmission electron microscopy (TEM, JEOL JEM-2010, Thailand) technique. The structural characterization and functional group identification of samples were analyzed by using Fourier transform infrared spectroscopy (FTIR, PerkinElmer Sciencific, Thailand) technique.

The mechanical property of all samples in the hardened state was carried out by compressive strength. The compressive strength of prismatic samples with dimensions of 150 × 30 × 30 mm^3 was studied in accordance with the ASTM C105 standard.

Results and Discussion

Figure 1 shows the result of X-ray diffraction (XRD) patterns of geopolymer, activated carbon, geopolymer/activated carbon with different activated carbon mole ratios of 0.001 and 0.003 %. The XRD patterns of activated carbon showed a broad peak appearing at 2θ of 24.15° and 43.44°, corresponding to the (002) and (100) plans in amorphous carbon [18,19]. In part of XRD pattern of geopolymer, the peak was located at 2θ of 21.78°, 26.80°, 50.28° and 60.51°, which can be indexed as quartz phase [7], whereas the peak was detected at 2θ of 13.51°, 34.07° and 42.04°, which can be assigned to mullite phase [7]. Furthermore, the sharp peak was located at 2θ of 23.73°, which can be identified as

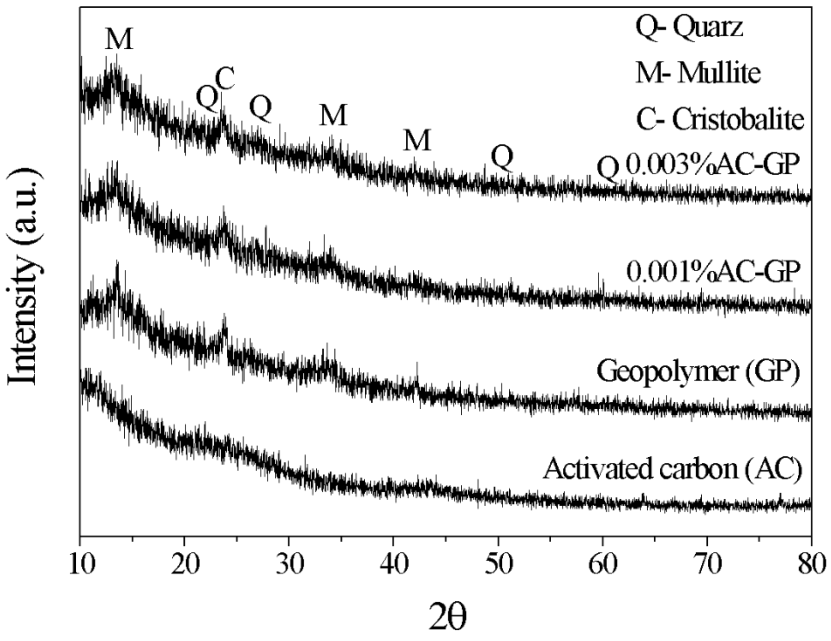

Fig. 1. XRD patterns of geopolymer, activated carbon, geopolymer/activated carbon with different activated carbon mole ratios of 0.001 and 0.003 %

the cristobalite phase in silica [7,20]. Moreover, it was found that the absence of alumina peak showed in XRD pattern, indicating that the alumina in geopolymer was in the amorphous phase [21]. For geopolymer/activated carbon with different activated carbon mole ratios of 0.001 and 0.003 %, the XRD peak was similar to pure geopolymer, which can be inferred that the addition of activated carbon content into geopolymer had no effect on the phase transition of geopolymer. In addition, it can be clearly observed that no activated carbon peak was emerged on geopolymer/activated carbon composite materials, owing to a very low content of activated carbon added into geopolymer.

The morphology of geopolymer, activated carbon, geopolymer/activated carbon with different activated carbon mole ratios of 0.001% and 0.003% was investigated through scanning electron microscopy (SEM), as shown in Fig. 2. Results showed that the morphology of geopolymer exhibited spherical-like structure, with average particle size of 50 to 100 nm approximately, as displayed in Fig. 2(a). Meanwhile, the activated carbon morphology was plate-like structure together with some pores distributed on the surface of activated carbon [22]. The size of pore diameters was about 1.4 to 1.9 μm corresponding to the macropore classification [23,24], as shown in Fig. 2(b). For composite materials, the morphology was consisted of the structures of geopolymer and activated carbon in composite materials, as represented in Fig. 2 (c,d).

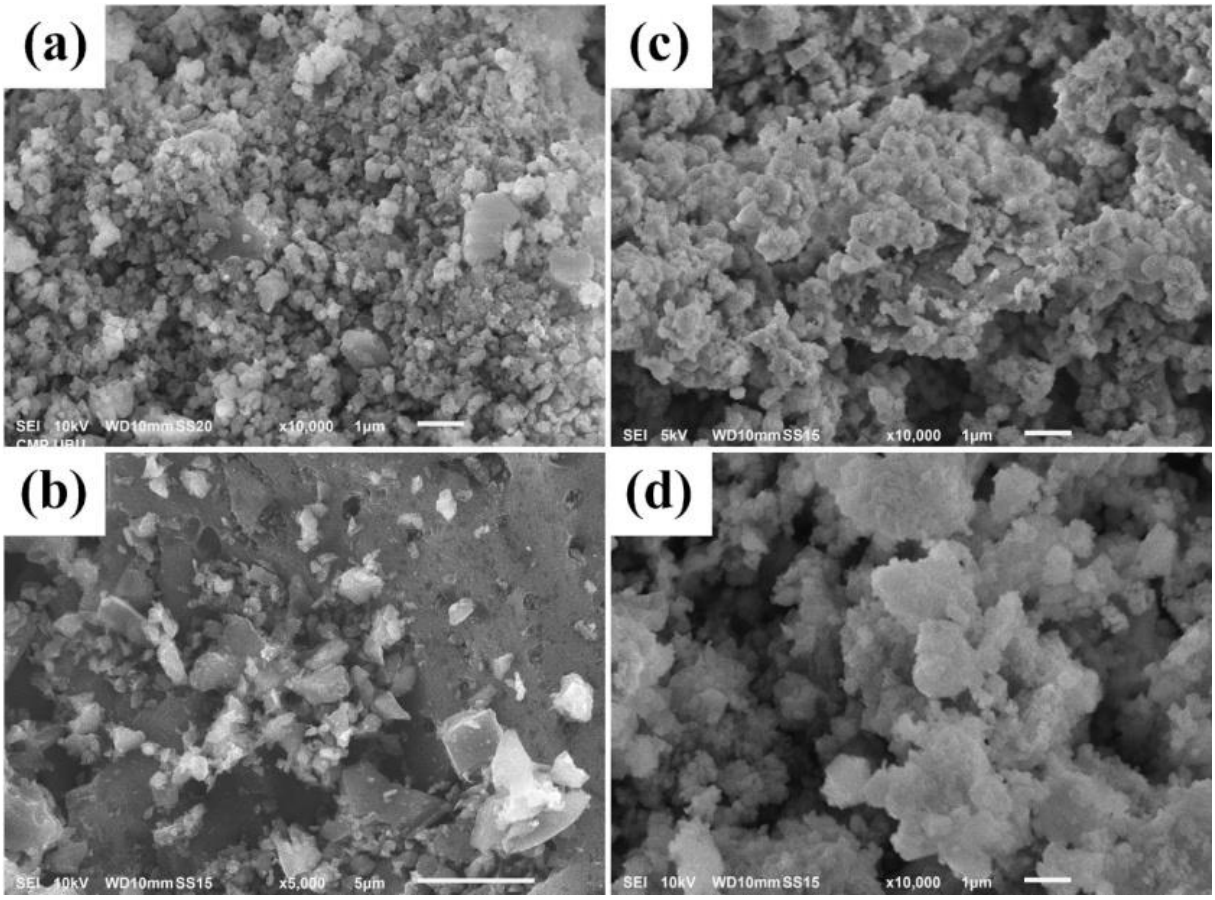

Fig. 2. SEM images of (a) geopolymer, (b) activated carbon and geopolymer/activated carbon with different activated carbon mole ratios of (c) 0.001 and (d) 0.003 %

To confirm the microstructure and particle size of geopolymer, activated carbon, geopolymer/activated carbon with different activated carbon mole ratios of 0.001% and 0.003%, transmission electron microscopy (TEM) was used, as shown in Fig. 3. The results of TEM image of geopolymer were spherical-like structure, with the average particle size of about 50 to 100 nm, as displayed in Fig. 3(a). In Figure 3 (b), TEM images of activated carbon were plate-like structure together with particle size of 20 to 100 nm approximately. For the composite materials, TEM images were composed of spherical-like and plate-like structures, as illuminated in Fig. 3(c,d). Therefore, it can be confirmed that the presence of activated carbon was in the geopolymer/activated carbon composite materials.

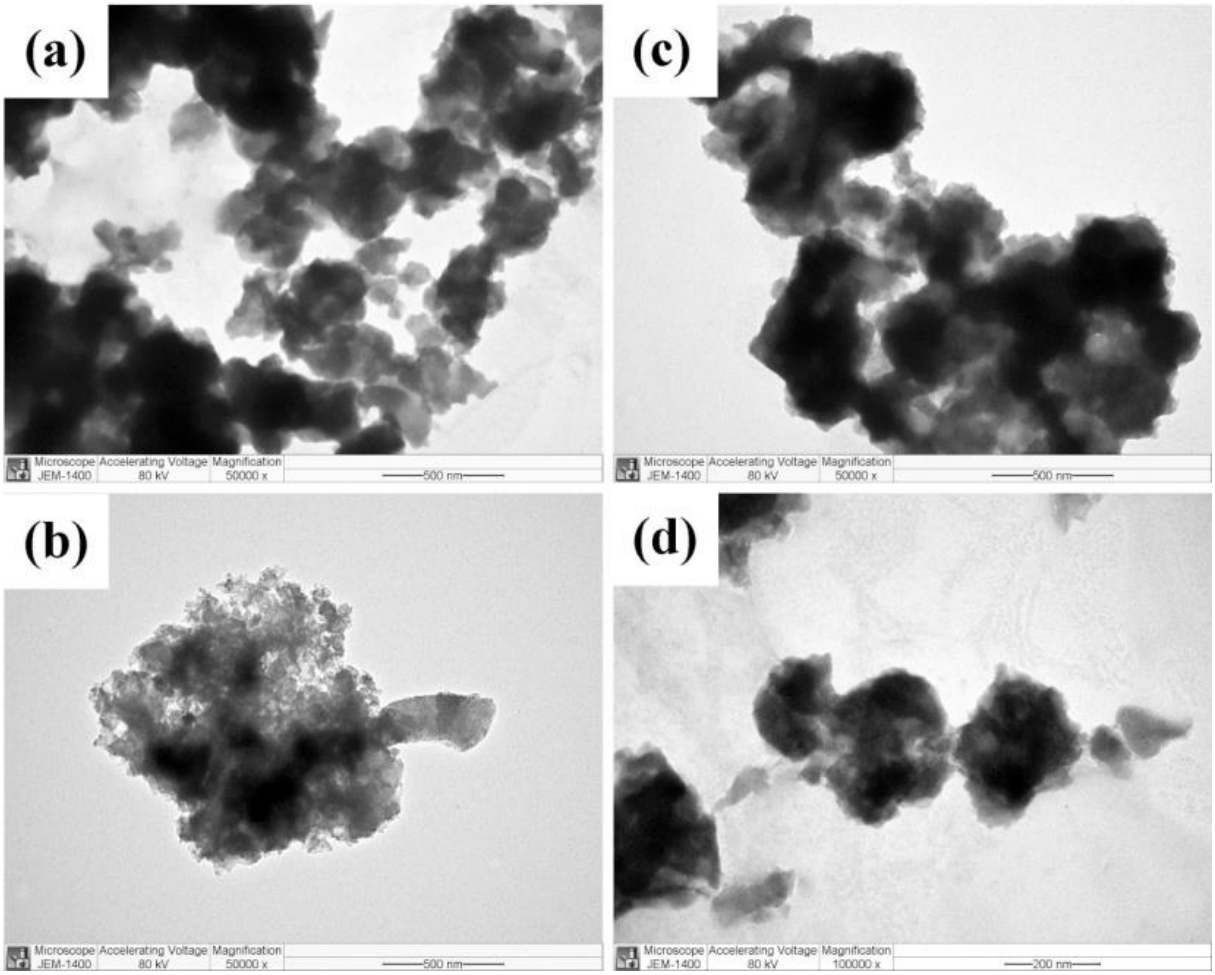

Fig. 3. TEM images of (a) geopolymer, (b) activated carbon and geopolymer/activated carbon with different activated carbon mole ratios of (c) 0.001 and (d) 0.003 %

The chemical structure and functional group of activated carbon, geopolymer and geopolymer/activated carbon with different activated carbon mole ratios of 0.001 and 0.003 % were studied by using Fourier transform infrared spectroscopy (FT-IR), as presented in Fig. 4. FT-IR spectra of activated carbon showed absorption bands at 3442 cm^{-1}, which might be due to the –OH stretching vibration [22]. The peaks occurred at 1558 cm^{-1} could be attributed to the N-H deformation vibration, C=C group or C=O stretching vibration in carbon [25], while the peaks at 2361 and 1208 cm^{-1} could be

due to the N-H and C-O stretching vibrations, respectively [25]. For FT-IR spectra of geopolymer, the peaks appeared at 3406 and 1443 cm^{-1} were ascribed to the O-H stretching vibration of absorbed H_2O molecules and C-O stretching vibration of CO_3^{2-} groups [26,27]. The peaks located at 977 cm^{-1} and 866 cm^{-1} were characterized as the Si-O-T (where T is tetrahedral Si or Al) asymmetric stretching vibration in geopolymer and O-C-O stretching vibration [28,29], respectively. The part of the peaks at 687 cm^{-1} to 425 cm^{-1} was corresponded to the Si-O-Si and Al-O-Si symmetric stretching vibrations, indicating the formation of amorphous aluminosilicate materials in geopolymer [30–32]. In part of FT-IR spectra of geopolymer/activated carbon with different activated carbon mole ratios of 0.001 and 0.003 %, the peaks were similar to the geopolymer. Furthermore, it can be observed that the peaks of geopolymer and /activated carbon composite materials occurred at 977 cm^{-1} were shifted to the lower wavenumbers (975 cm^{-1}) after geopolymerization reaction [33,34]. The shifting and reduction of peaks in the geopolymer and /activated carbon composite materials might be due to the interaction of aluminum atoms and the formation of poly (sialate-siloxo) chain in geopolymer structure [34,35].

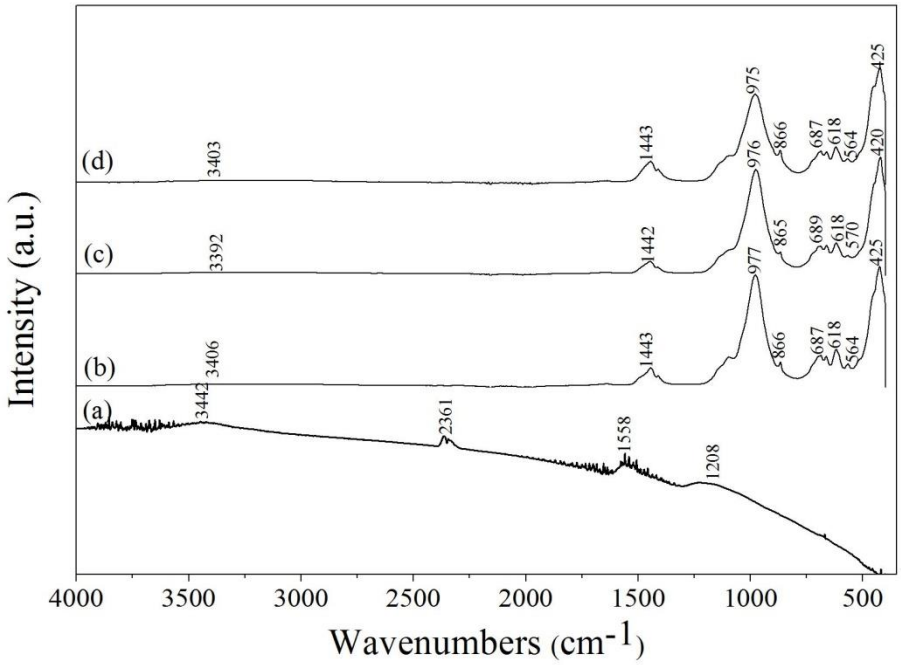

Fig. 4. FT-IR spectra of activated carbon, geopolymer and geopolymer/activated carbon with different activated carbon mole ratios of 0.001 and 0.003 %

The compressive strengths of geopolymer and geopolymer/activated carbon composite materials with different activated carbon mole ratios of 0.001 and 0.003 % were shown in Fig. 5. From experimental results, the compressive strength of geopolymer was 12.79 MPa, while the geopolymer/activated carbon composite materials with different activated carbon mole ratios of 0.001 and 0.003 % were 16.09 and 10.93 MPa, respectively. The obtained results were found that the concentration of 0.001 mol. % activated carbon added into the geopolymer showed the highest strength. While the concentration of 0.003 mol. % activated carbon was introduced into the geopolymer, the

strength of geopolymer was decreased. Therefore, it was concluded that the concentration of activated carbon added into geopolymer had an effect on the strength of geopolymer, the 0.001 mol.% activated carbon loaded into the geopolymer was a suitable concentration to function as a bone substitute material in the future.

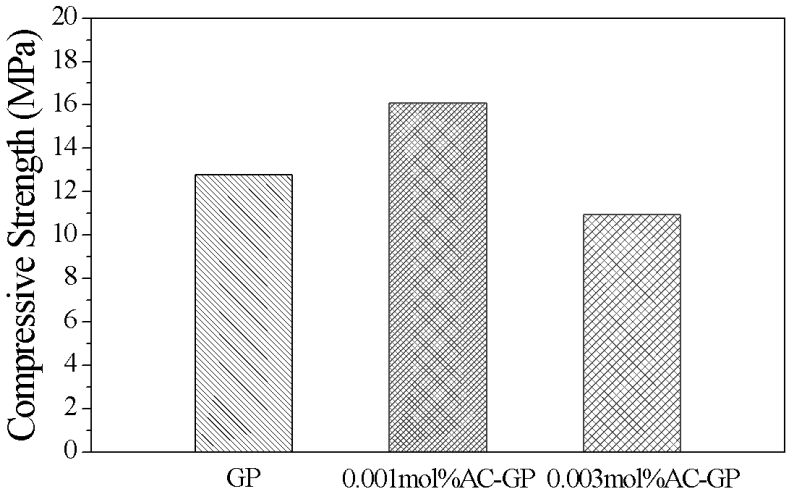

Fig. 5. Compressive strength of geopolymer and geopolymer/activated carbon composite materials with different activated carbon mole ratios of 0.001 and 0.003 %

Conclusions

In summary, geopolymer/activated carbon composite materials were successfully synthesized from metakaolin using a NaOH alkaline activator solution as a binder. The resulting geopolymer/activated carbon composite materials exhibited an amorphous phase. The composite materials consisted of spherical-like geopolymer and plate-like activated carbon, with an average particle size ranging from 20 to 100 nm. The FTIR band of the geopolymer/activated carbon composite materials, after the geopolymerization reaction, shifted slightly from 977 to 975 cm^{-1}. This shift could be attributed to the interaction of the functional groups of aluminum atoms and the increased cross-linking within the geopolymer structure. The sample with 0.001 % activated carbon demonstrated the highest strength compared to the other samples.

CRediT authorship contribution statement

A. Moonphukhiao: writing – review & editing; **Buagun Samran:** writing – original draft; **Saranyoo Chaiwichian:** writing – review & editing; writing – original draft; investigation.

Conflict of interest

The authors declare that they have no conflict of interest.

References

1. Florencio-Silva R, da Sasso GRS, Sasso-Cerri E, Simões MJ, Cerri PS. Biology of bone tissue: Structure, function, and factors that influence bone cells. *BioMed Research International*. 2015;1: 421746.
2. Ricciotti L, Apicella A, Perrotta V, Aversa R. Geopolymer materials for bone tissue applications: recent advances and future perspectives. *Polymers*. 2023;15(5): 1087.
3. Huang H, Liu X, Wang J, Suo M, Zhang J, Sun T, Wang H, Liu C, Li Z. Strategies to improve the performance of polyetheretherketone (PEEK) as orthopedic implants: from surface modification to addition of bioactive materials. *Journal of Materials Chemistry B*. 2024:12(19): 4533–4552.
4. Rodriguez J, Mónica Mandalunis P. A review of metal exposure and its effects on bone health. *Journal of Toxicology*. 2018;2018(1): 4854152.
5. Swanepoel JC, Strydom CA. Utilization of fly ash in a geopolymeric material. *Applied Geochemistry*. 2002;17(8): 1143–1148.
6. Davidovits J. Geopolymers: inorganic polymeric new materials. *Journal of Thermal Analysis and Calorimetry*. 1991;37(8): 1633–1656.
7. Hwang CL, Huyn TP. Effect of alkali-activator and rice husk ash content on strength development of fly ash and residual rice husk ash-based geopolymers. *Construction and Building Materials*. 2015;101: 1–9.
8. Cui YF, Qu SH, Bao JW, Zhang P. Bond performance of steel bar and fly ash-based geopolymer concrete in beam end tests. *Polymers*. 2020;14: 2012.
9. Baqi HJ. Assessment of the Effects of Boron Nitride Nanoplatelets Reinforcement on the Physical and Mechanical Properties of the Geopolymer Prepared by Natural Kaolinite: An in Vitro Study. *Dental Hypotheses*. 2024:15(1): 11–13.
10. Kudłacik-Kramarczyk S, Drabczyk A, Figiela B, Korniejenko K. Geopolymers: Advanced Materials in Medicine, Energy, Anticorrosion and Environmental Protection. *Materials*. 2023:16(23): 7416.
11. Jamaludin L, Razak RA, Abdullah MMAB, Vizureanu P, Bras A, Imjai T, Sandu AV, Abd Rahim SZ, Yong HC. The suitability of photocatalyst precursor materials in geopolymer coating applications: a review. *Coatings*. 2022;12(9): 1348.
12. Radhi HAA, Ahmad MA. Biological Test of Porous Geopolymer as a Bone Substitute. *Journal of Medicinal and Chemical Sciences*. 2023;6: 710–719.
13. Provis JL, Duxson P, van Deventer JSJ. The role of particle technology in developing sustainable construction materials. *Advanced Powder Technology*. 2010;21(1): 2–7.
14. Casagrande Paim T, Bertaco I, Naasani LS, Buchner S, Kovářík T, Hájek J, Wink MR. Hierarchically porous bioceramics based on geopolymer-hydroxyapatite composite as a novel biomaterial: Structure, mechanical properties and biocompatibility evaluation. *Applied Materials Today*. 2023:33: 101875.
15. Kriven WM, Leonelli C, Provis JL, Boccaccini AR, Attwell C, Ducman VS, Ferone C, Rossignol S, Luukkonen T, Van Deventer JSJ, Emiliano, JV, Lombardi JE. Why geopolymers and alkali-activated materials are key components of a sustainable world: A perspective contribution. *Journal of the American Ceramic Society*. 2024:107(8): 5159–5177.
16. Pimraksa K, Setthaya N, Thala M, Chindaprasirt P, Murayama M. Geopolymer/Zeolite composite materials with adsorptive and photocatalytic properties for dye removal. *Plos one*. 2020;15(10): e0241603.
17. Wang X, Hu Z, Chen Y, Zhao G, Liu Y, Wen Z. A novel approach towards high-performance composite photocatalyst of TiO_2 deposited on activated carbon. *Applied Surface Science*. 2009;255: 3953–3958.
18. Xing BL, Shi CL, Zhang CX, Yi GY, Chen LJ, Guo H, Huang GX, Cao JL. Preparation of TiO_2/Activated Carbon Composites for Photocatalytic Degradation of RhB under UV Light Irradiation. *Journal of Nanomaterials*. 2016;2016(1): 8393648.
19. Lee HM, Lee BH, An KH, Park SJ, Kim BJ. Facile preparation of activated carbon with optimal pore range for high butane working capacity. *Carbon Letters*. 2020;30: 297–305.
20. Xu W, Lo TY, Memon SA. Microstructure and reactivity of rich husk ash. *Construction and Building Materials*. 2012;29: 541–547.
21. He J, Jie Y, Zhang J, Yu Y, Zhang G. Synthesis and characterization of red mud and rice husk ash-based geopolymer composites. *Cement* and *Concrete Composites*. 2013;37: 108–118.
22. Moyo M, Nyamhere G, Sebata E, Guyo U. Kinetic and equilibrium modelling of lead sorption from aqueous solution by activated carbon from goat dung. *Desalination and Water Treatment*. 2016;57(2): 765–775.

23. Wang YW, Duan YH, Liang X, Tang L, Sun L, Wang RR, Wei SH, Huang HN, Yang PH, Hu HN. Hierarchical porous activated carbon derived from coconut shell for ultrahigh-performance supercapacitors. *Molecules.* 2023;28(20): 7187.
24. Wang Y, Lu W, Xu X, Pang F, Feng X, Zhang X, Zeng Y, Yang Z, Wang R, Yang P. Ternary-doped hierarchical porous carbons derived from durian kernel as electrode materials for efficient energy storage devices. *Diamond and Related Materials.* 2022;130: 109451.
25. Liu Y, Liu XH, Dong WP, Zhang LL, Kong Q, Wang WL. Efcient adsorption of sulfamethazine onto modifed activated carbon: a plausible adsorption mechanism. *Scientific Reports.* 2017;7: 12437.
26. Azhar NSDM, Zainal FF, Abdullah MMAB. Bonding and phases analysis of geopolymer materials. *IOP* Conference *Series*: *Materials Science and Engineering.* 2020;957: 012052.
27. Mužek MN, Svilović S, Zelić J. Fly ash-based geopolymeric adsorbent for copper ion removal from wastewater. *Desalination* and *Water Treatment.* 2014;52: 2519–2526.
28. Bakharev T. Resistance of geopolymer materials to acid attack. *Cement and Concrete Research.* 2005;35(4): 658–670.
29. Guo X, Pan X. Effects of steel slag on mechanical properties and mechanism of fly ash-based geopolymer. *Journal of Materials in Civil Engineering.* 2020;32(2): 04019348.
30. Villa C, Pecina ET, Torres R, Go´mez L. Geopolymer synthesis using alkaline activation of natural zeolite. *Construction and Building Materials.* 2010;24(11): 2084–2090.
31. Maiti M, Sarkar M, Maiti S, Malik MA, Xu S. Modification of geopolymer with size controlled TiO_2 nanoparticle for enhanced durability and catalytic dye degradation under UV light. *Journal of Cleaner Production.* 2020;255: 120183.
32. Sindhunata Van Deventer JSJ, Lukey GC, Xu H. Effect of curing temperature and silicate concentration on fly-ash-based geopolymerization. *Industrial & Engineering Chemistry Research.* 2006;45: 3559–3568.
33. Van Jaarsveld JGS, Van Deventer JSJ. Effect of the alkali metal activator on the properties of fly ash-based geopolymers. *Industrial & Engineering Chemistry Research.* 1999;38: 3932–3941.
34. Chen L, Wang Z, Wang Y, Feng J. Preparation and properties of alkali activated metakaolin-based geopolymer. *Materials.* 2016;9(9): 767.
35. Cheng-Yong H, Yun-Ming L, Abdullah MMAB, Hussin K. Thermal resistance variations of fly ash geopolymers: foaming responses. *Scientific Reports.* 2017;7(1): 45355.